

How Low Can You Go? Low Densities of Poly(ethylene glycol)
Surfactants Attract Stealth Proteins

Peer-reviewed author version

SENECA, Senne; Simon, Johanna; Weber, Claudia; Ghazaryan, Arthur;
ETHIRAJAN, Anitha; Mailaender, Volker; Morsbach, Svenja & Landfester, Katharina
(2018) How Low Can You Go? Low Densities of Poly(ethylene glycol) Surfactants
Attract Stealth Proteins. In: MACROMOLECULAR BIOSCIENCE, 18(9) (Art N° 1800075).

DOI: 10.1002/mabi.201800075

Handle: <http://hdl.handle.net/1942/27509>

1 **How low can you go? Low densities of poly(ethylene glycol) surfactants attract**
2 **stealth proteins**

3 S. Seneca,^{a,c} J. Simon,^c C. Weber,^c A. Ghazaryan,^c A. Ethirajan,^{a,b} V. Mailaender,^{c,d} S. Morsbach^c
4 and K. Landfester^c

5 a. Institute for Materials Research (IMO), Hasselt University, Wetenschapspark 1 and Agoralaan
6 D, 3590 Diepenbeek, Belgium.

7 b. IMEC, associated lab IMOMECE, Wetenschapspark 1, 3590 Diepenbeek, Belgium.

8 c. Max Planck Institute for Polymer Research, Ackermannweg 10, 55128 Mainz, Germany.

9 d. Department of Dermatology, University Medical Center of the Johannes Gutenberg-University
10 Mainz, Langenbeckstrasse 1, 55131 Mainz, Germany.

11 Email: morsbachs@mpip-mainz.mpg.de

12 **Abstract**

13 It is now well-established that the surface chemistry and “stealth” surface functionalities such as
14 poly(ethylene glycol) (PEG) chains of nanocarriers play an important role to decrease unspecific
15 protein adsorption of opsonizing proteins, to increase the enrichment of specific stealth proteins
16 and to prolong the circulation times of the nanocarriers. At the same time, PEG chains are used to
17 provide colloidal stability for the nanoparticles. However, it is not clear how the chain length and
18 density influences the unspecific and specific protein adsorption keeping at the same time the
19 stability of the nanoparticles in a biological environment. Therefore, this study aims at
20 characterizing the protein adsorption patterns depending on PEG chain length and density to define
21 limits for the amount of PEG needed for a stealth effect by selective protein adsorption as well as

1 colloidal stability during cell experiments. PEG chains were introduced using of the PEGylated
2 Lutensol AT surfactants, which allows easy modification of the nanoparticle surface. Our findings
3 indicate that a specific enrichment of stealth proteins already occurs at low PEG concentrations;
4 for the decrease of unspecific protein adsorption and lastly the colloidal stability a full surface
5 coverage is advised.

6 **Introduction**

7 In recent years, understanding of the surface chemistry of nanoparticles and especially the role of
8 “stealth” functionalities gained much interest to determine the nanoparticle behavior in biological
9 media and their interaction with blood plasma components such as proteins and afterwards with
10 different cells.^[1-3] To this extent, poly(ethylene glycol) (PEG) chains grafted to the surface of
11 nanoparticles have been extensively studied to reduce overall protein adsorption, prolong the
12 circulation time of nanocarriers and decrease non-specific cellular uptake, especially by cells of the
13 mononuclear phagocyte system (i.e. macrophages).^[4-7] Recent investigations by *Schöttler et al.*
14 revealed that next to the reduction in non-specific protein adsorption, the type of proteins
15 constituting the protein corona of nanoparticles is most important to trigger the highly desired
16 “stealth effect”.^[8] More particularly, the specific enrichment of distinct “don’t-take-me-up”
17 proteins, and especially the high abundance of clusterin (apolipoprotein J) and apolipoprotein A1
18 in the protein pattern of PEGylated nanoparticles, plays a decisive role to prevent undesirable
19 uptake by cells of the immune system.^[9]

20 Most investigations on PEGylated nanoparticles and substrates describe the presence of a critical
21 balance between the protein adsorption behavior and the conformation of PEG chains (in terms of
22 PEG molecular weight, polymer chain architecture, and the surface density of PEG coating).^[10, 11]
23 A general consensus exists that increasing grafting densities result in a more efficient reduction of

1 overall protein adsorption.^[12, 13] Mostly, the PEGylation density is described according to the two
2 main conformations PEG chains can take when grafted onto a surface: “mushroom” (low PEG
3 grafting density) and “brush” (high PEG grafting density).^[14, 15] Very recently, detailed attempts
4 by *Bertrand et al.* demonstrated that PEGylation surface densities of approximately 20
5 poly(ethylene glycol) chains (molecular weight of 5 kDa) per 100 nm² prolong circulation times,
6 irrespective of the size of the nanoparticles. Moreover, they showed that the specific adsorption of
7 apolipoproteins, already at low PEG surface coverages, could prolong circulation times, whereas a
8 predominant role of low-density-lipoprotein receptors on the clearance of nanoparticles,
9 independent of PEGylation density, was demonstrated as well.^[16] Despite these investigations on
10 the existence of a certain threshold of PEG grafting density sufficient to allow a significant
11 reduction in protein adsorption, no conclusive standard really exists as to what surface density and
12 PEG chain length is needed to accomplish a stealth effect in terms of immune cell uptake via
13 physically adsorbed PEG chains.^[10, 13] Additionally, characterizing the protein corona composition
14 originating from PEGylated nanoparticles as a function of PEG chain length and surface density is
15 missing, thereby coming up short on the second prerequisite to achieve the stealth effect, namely
16 the specific enrichment of dysopsonizing proteins such as clusterin.

17 Whereas most articles report on the covalent attachment of PEG chains on surfaces, investigations
18 on the non-covalent attachment of PEG chains are limited. One of the first reports addressing the
19 adsorption of PEG chains by Malmsten et al. has shown, however, that the protein rejecting
20 capacity of physically adsorbed PEG chains is similar to the efficient protein rejection at
21 sufficiently high chain density of covalently grafted PEG layers.^[17] Only recently, non-covalent
22 PEGylation was established by the formation of a protein-polymer consisting out of a hexavalent
23 lectin and a fucose-capped PEG. In general, this method would allow for incorporation of glycol-
24 PEG functionalities in proteins with an engineered sugar-binding site.^[18] It is worth mentioning

1 that theoretical approaches to describe the effect of modulating size and grafting density of PEG
2 on the plasma adsorption behavior of PEGylated surfaces are in concordance with experimental
3 studies.^[19, 20] For example, Lee and Larson performed coarse-grained molecular dynamic
4 simulations to predict and explain the different behaviours of human serum albumin on PEGylated
5 lipid bilayers with different grafting densities.^[21]

6 Recently, our research group has identified the use of biocompatible polymer surfactant molecules
7 like poly(phosphoester)s (PPEs) to trigger a similar stealth effects as PEG.^[22] The as-synthesized
8 non-ionic PPE-surfactants could be physically adsorbed as nanoparticle coating, thereby
9 circumventing the tedious synthesis steps to allow the covalent attachment of PEG on the
10 nanoparticle surface and still providing colloidal stability. Moreover, by adjusting their length (of
11 lyophilic and hydrophilic parts) and hydrophilicity, tailored surfactants with desirable protein
12 adsorption properties could be achieved.^[22-24] In addition, Winzen et al. showed that small
13 concentration differences of surfactant molecules present at the surface of nanoparticles possess a
14 strong influence on protein adsorption behavior.^[25]

15 In this work, polymeric polystyrene nanoparticles coated with various types (chain length) of the
16 PEG-based surfactant Lutensol (Lut) were investigated with respect to their protein corona
17 composition and nanoparticle-cell interactions by varying the PEGylation properties. Lutensol is
18 composed of a C16-C18 hydrophobic saturated fatty alcohol and a hydrophilic PEG block.
19 Therefore, it has been postulated that it can be applied to reduce unspecific protein adsorption and
20 enhance the enrichment of particularly clusterin as main protein in the protein corona pattern. The
21 aim of this study is to provide important information on the minimum amount of PEG grafting
22 density and chain length, necessary to obtain a stealth behaviour and still provide sufficient stability
23 to the nanoparticles.

1 **Results and Discussion**

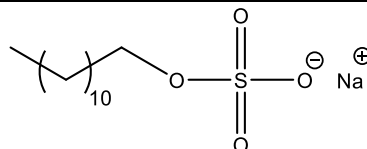
2 **Nanoparticle characterization and Lutensol adsorption characteristics**

3 In this study, model polystyrene nanoparticles prestabilized with different stabilizing agents (either
4 non-ionic Lut AT50 or anionic SDS surfactant) were synthesized employing mini-emulsion
5 polymerization using a microfluidizer setup for the homogenization and development of narrowly
6 size-distributed nanoparticles. Since the purpose of this study is to characterize the influence of
7 PEGylation surface properties (in terms of PEG surface coverage and PEG chain length), each
8 sample was thoroughly purified. To ensure that the minimal surfactant concentration necessary to
9 preserve stable nanoparticles was reached, the usual purification time was extended. As a control,
10 the surface tension of the air-water interface was measured and compared with the value for pure
11 water (73.08 mN m^{-1}). Furthermore, the particles were characterized with respect to their size,
12 surface charge and morphology using dynamic light scattering, zeta potential measurements and
13 electron microscopy (see Table 1 and Figure S1-S2). The obtained size difference of the particle
14 systems is due to different optimum surfactant concentrations in the synthesis resulting from the
15 different stabilization mechanism (ionic vs. steric stabilization).

16 For the SDS-stabilized nanoparticles a high air-water surface tension of $72.40 \pm 0.06 \text{ mN}$
17 m^{-1} was obtained. The highest surface tension for Lut-stabilized nanoparticles was 56.26 ± 0.09
18 mN m^{-1} . Removing additional surfactant resulted in aggregate formation, indicating that the
19 concentration of surfactant present at the nanoparticle surface was too low to stabilize all particles.
20 Those highly purified samples were taken as reference samples because of minimal surfactant
21 remaining. It should be mentioned that the surface tension of the Lut-stabilized particle dispersion
22 is not as close to the reference value of water as compared to the surface tension of the SDS-
23 stabilized particle dispersion after extensive washing steps. It seems that Lut has a strong tendency

1 to be present at the air-water interface and already minimal amounts of free Lut will readily
 2 accumulate there (as shown earlier by Winzen et al.).^[25]

3 Table 1 Physicochemical characteristics of model polystyrene nanoparticles synthesized via
 4 emulsion polymerization, using a microfluidizer setup for the homogenization.

	Lutensol AT 50-stabilized	SDS-stabilized
Structure of surfactant	 $x = 15 - 17$	
Diameter / nm	272 ± 27	96 ± 10
Zeta Potential / mV	-6 ± 1	-42 ± 1
Surface Tension / mN m ⁻¹	56.26 ± 0.09	72.40 ± 0.06

5

6 After synthesis and extensive purification of the polystyrene nanoparticles, the Lut-stabilized
 7 polystyrene particles were functionalized with different Lut AT type surfactants, which differ in
 8 chain length of their hydrophilic PEG block (where the number following AT in the name refers to
 9 the number of PEG units in the hydrophilic chain, see Table 1). To investigate the influence of
 10 PEG chain length and surface coverage, the particles were functionalized according to 30%, 60%
 11 and 90% surface coverage relative to the maximum binding sites of short (Lut AT11 and 25),
 12 medium (Lut AT50) and long (Lut AT80) PEG chains each. The functionalization was performed
 13 after determining the maximum amount of surfactant molecules bound per purified nanoparticle
 14 using isothermal titration calorimetry (ITC). ITC can be applied to measure enthalpy changes, and
 15 therefore the thermodynamic parameters of surfactant adsorption, arising from the interaction
 16 between different components directly. By titrating a purified nanoparticle dispersion with an
 17 aqueous solution of each Lutensol surfactant and analysing the heat changes of the adsorption
 18 according to an independent binding model, information can be obtained with respect to the

1 association constant K_a , binding enthalpy ΔH , and stoichiometry n of surfactant molecules per
 2 nanoparticle. To exclude dilution effects because of titration, a blank titration run was performed
 3 (titration of surfactant into water) and the resulting heats were subtracted from the nanoparticle
 4 titrations. The obtained binding parameters for each surfactant are summarized in Table 2. The
 5 integrated normalized heats together with the independent binding fits as a function of molecular
 6 ratio of surfactant molecules per particle are presented in Figure S3-S4.

7 Table 2 Lutensol AT type surfactant adsorption parameters on Lutensol AT 50-stabilized
 8 polystyrene nanoparticles obtained from ITC measurements applying an independent binding fit
 9 model. Mean values of triplicates are given with their standard deviation.

#	M_w^a / g mol ⁻¹	K_a / L mol ⁻¹	ΔH / kJ mol ⁻¹	ΔS / J K ⁻¹ mol ⁻¹	ΔG / kJ mol ⁻¹	n	occupied area/nm ² per surfactant molecule
AT 11	740	$(2.0 \pm 0.3) \cdot 10^4$	-9.1 ± 0.9	51.7 ± 4.2	-24.5 ± 0.4	$267,514 \pm 7485$	0.87
AT 25	1,360	$(2.6 \pm 0.9) \cdot 10^4$	-10.1 ± 1.3	50.1 ± 7.2	-25.0 ± 0.9	$95,963 \pm 1936$	2.42
AT 50	2,460	$(6.3 \pm 0.6) \cdot 10^6$	16.1 ± 0.1	184.2 ± 1.3	-54.9 ± 0.4	$18,048 \pm 34$	12.21
AT 80	3,780	$(6.7 \pm 1.6) \cdot 10^6$	18.1 ± 0.6	191.3 ± 0.1	-38.9 ± 0.6	$15,785 \pm 39$	14.72

10 ^a As given by the supplier.

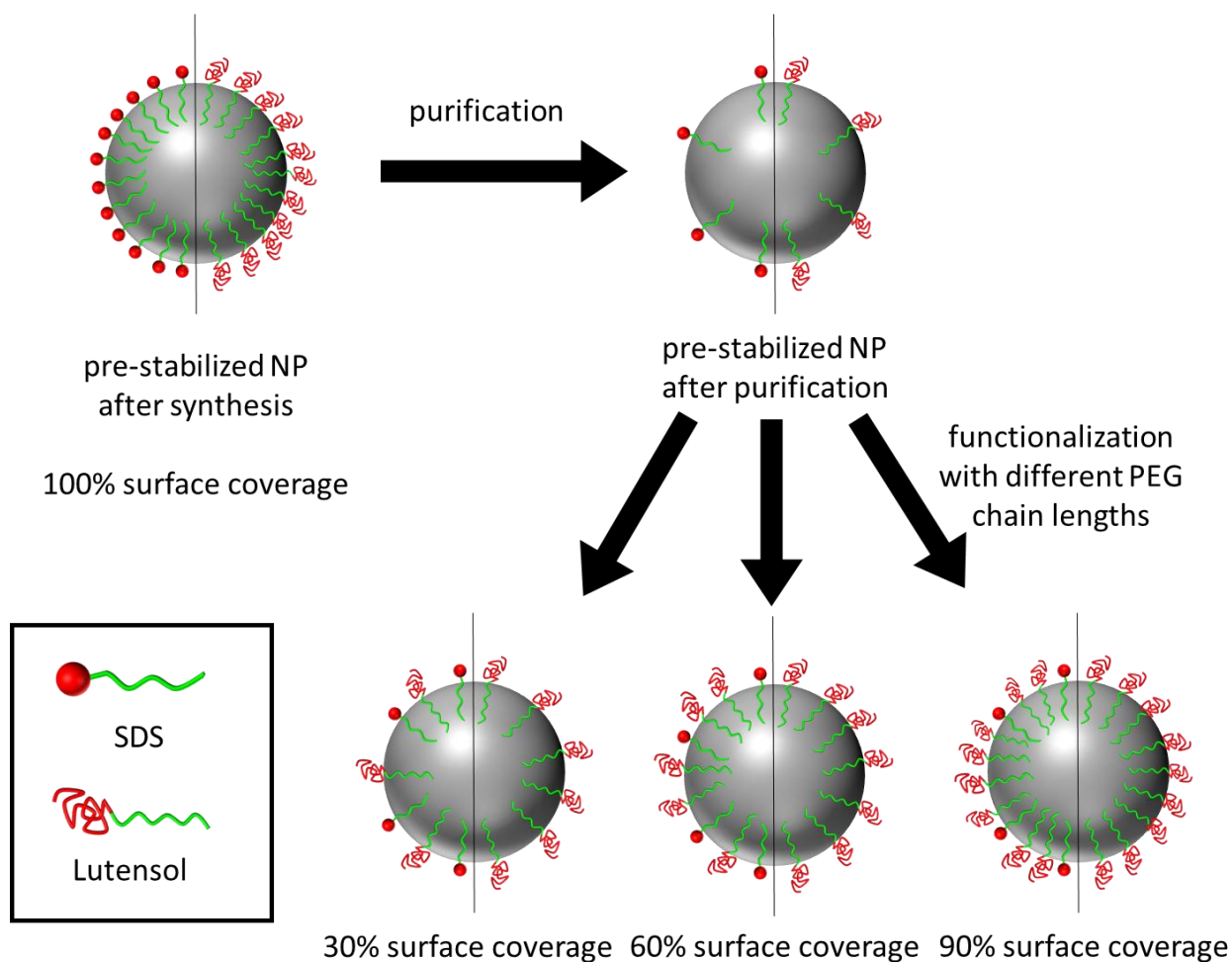
11

12 Interestingly, the surfactant binding affinity increases with increasing length of the PEG
 13 block, what first seems to be counterintuitive because of a better surfactant solubility. However,
 14 this effect was already found for other nonionic surfactants^[22] and most likely originates from an
 15 interaction of the nanoparticle surface with not only the hydrophobic, but also the hydrophilic chain
 16 of the surfactants when they become long enough to arrange in a coiled or ‘mushroom’
 17 conformation. This proposed change in surfactant conformation and interaction with the NP surface
 18 is also supported by the change from an exothermic to an endothermic adsorption process.
 19 According to the increasing entropy gain, more water molecules from the hydration shells of longer

1 PEG chains will be released into the solution, so that hydrophobic interaction between the $-\text{CH}_2-$
2 CH_2- moieties and PS surface can take place.

3 From the obtained stoichiometry, the occupied area per molecule of the different surfactant
4 types was calculated from the nanoparticle surface area and the average number of surfactant
5 molecules adsorbed on the nanoparticle surface as obtained from ITC measurements. As expected,
6 the surface area of surfactant molecules increases almost linearly with increasing chain length of
7 the hydrophilic PEG block. These results suggest a strong relationship of the packing of surfactant
8 molecules on the surface of nanoparticles depending on the chain length of the hydrophilic part.
9 Hereby, it can be assumed that shorter surfactant molecules tend to arrange themselves linearly
10 packed on the nanoparticle surface, whereas longer surfactant molecules tend to coil up thereby
11 increasing their surface area.

12 After determining the average number of surfactant molecules adsorbing on the
13 nanoparticle surface (which corresponds to 100% surface coverage) for each surfactant, the
14 purified polystyrene particles were functionalized according to 30%, 60% or 90% surface coverage
15 of short, medium and long PEG chains each (see Figure 1).



1

2 **Figure 1** Schematic illustration of the experimental workflow. **Note that hydrophobic tails of surfactants**

3 **are drawn as extending into the particle material for visualization reasons, which does not necessarily**

4 **represent the actual conformation after surfactant addition (a flat-on adsorption is more likely).**

5 To verify whether the functionalization was successful, $^1\text{H-NMR}$ spectroscopy analysis was

6 performed on the purified as well as the differently functionalized particles in D_2O (Figure S5).

7 For this purpose, an internal standard of dimethyl sulfoxide (DMSO) was used as a reference to

8 which the integrated PEG peak was compared. Since Lutensol AT50 was used as stabilizing agent

9 during the synthesis process, it was only possible to directly compare the resulting integrals with

10 respect to Lutensol AT50-functionalized polystyrene nanoparticles with different surface

11 coverages. The signal obtained for the hydrophilic PEG chain ($-\text{O}-\text{CH}_2$ -groups) was integrated

1 from $\delta = 3.2$ to 3.8 ppm since the peak is broadened due to immobilization of the Lutensol on the
2 nanoparticle surfaces.

3 The DMSO internal standard was integrated from $\delta = 2.5$ to 2.7 ppm and its value normalized to
4 1. Increasing amounts of Lutensol resulted in an increased integral of the Lutensol peak compared
5 to the internal standard without a significant sharpening of the peak, which would indicate higher
6 amounts of free Lutensol.

7 Therefore, it was assumed that the functionalization of the polystyrene nanoparticles was
8 successful and that different surface coverages were obtained. However, it should be noted that the
9 addition of surfactant molecules to a solution is always a system in equilibrium. This implies that
10 some amounts of surfactant molecules are assumed to stay in solution and a higher amount will
11 adsorb on the nanoparticle surface. Moreover, similar analysis of the NMR data for Lutensol AT11,
12 25 and 80 as surface functionalities indicated successful functionalization of nanoparticles to obtain
13 different surface coverages (Figure S6).

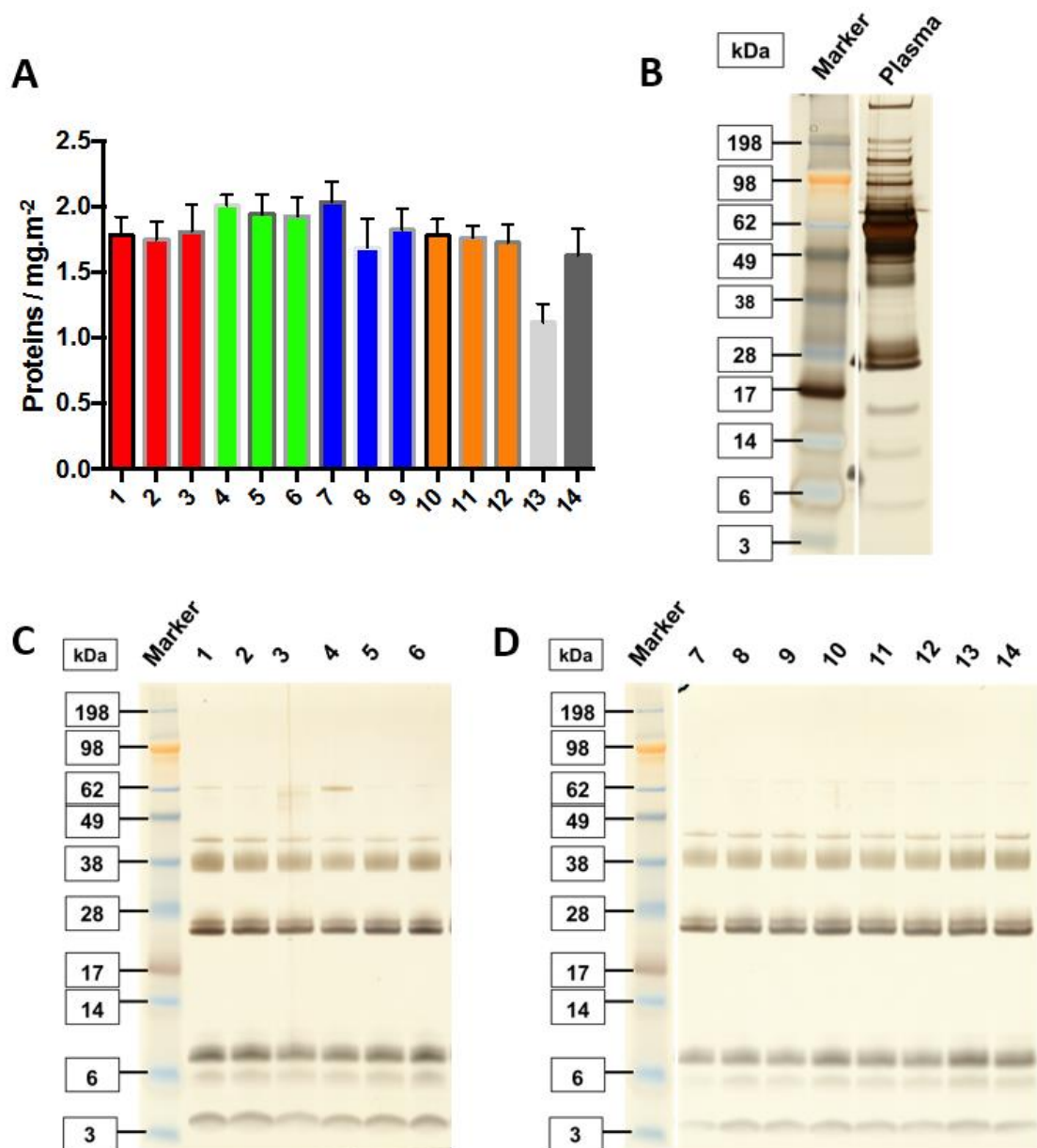
14 Functionalization of SDS-prestabilized nanoparticles was performed based on the information
15 obtained about the occupied surface area per surfactant molecule from the ITC measurements of
16 the Lutensol AT50-stabilized nanoparticles.

17

18 **Protein corona evaluation**

19 To determine the potential “stealth” effect of Lutensol as surface functionality, and the effect of
20 PEG chain length and surface coverage, the protein corona of Lutensol-stabilized polystyrene
21 nanoparticles was investigated (Figure 2). For this purpose, the nanoparticles were incubated with
22 human citrate-stabilized plasma^[26] and free proteins were removed by performing three
23 centrifugation and washing steps. Afterwards, the strongly associated proteins (hard protein

1 corona)^[27] were removed from the surface of the nanoparticle following a treatment with SDS and
 2 Tris-HCl. The collected proteins were investigated quantitatively using a colorimetric protein assay
 3 (Pierce 660 nm protein assay) and qualitatively with SDS-PAGE. In addition, the zeta potential
 4 was measured before and after protein incubation (Table S1.1).



5
 6 **Figure 2** Quantitative characterization of the hard protein corona pattern of Lutensol-stabilized Lutensol-
 7 functionalized polystyrene nanoparticles via a Pierce 660 nm protein assay (A) in combination with
 8 qualitative analysis via SDS-PAGE (C and D). Proteins were detached from the nanoparticle surface after

1 multiple washing steps using an SDS Tris-HCl solution. Pure plasma (B) is given as a reference. 1) Lut
2 AT11, 30% surface coverage; 2) Lut AT11, 60% surface coverage, 3) Lut AT11, 90% surface coverage, 4)
3 Lut AT25, 30% surface coverage, 5) Lut AT25, 60% surface coverage, 6) Lut AT25, 90% surface coverage,
4 7) Lut AT50, 30% surface coverage, 8) Lut AT50, 60% surface coverage, 9) Lut AT50, 90% surface
5 coverage, 10) Lut AT80, 30% surface coverage, 11) Lut AT80, 60% surface coverage, 12) Lut AT80, 90%
6 surface coverage; 13) unpurified Lut-stabilized PS NPs, and 14) purified Lut-stabilized PS NPs.

7 In contrast to initial expectations, no remarkable differences in protein adsorption behavior
8 were observed among the different Lutensol-functionalized polystyrene nanoparticles when
9 Lutensol was used as stabilizing agent during the synthesis process. It seems that neither the chain
10 length of the hydrophilic PEG block, nor the surface coverage exhibits a profound impact on the
11 adsorption behavior (protein mass and pattern) of proteins on these particles. The only exception
12 that can be observed is with the unpurified nanoparticle sample, where the decreased protein
13 adsorption might be a result of Lutensol remaining in solution that already interacts with a
14 significant protein amount. SDS-PAGE analysis confirms the quantitative results from the protein
15 assay. It can be observed that the protein pattern of all examined nanoparticles is very different
16 from the pattern of pure plasma without any nanoparticles. Within the pure plasma sample, the
17 most dominant protein bands in pure plasma can be identified as proteins with a high plasma
18 concentration: HSA ($\sim 44 \text{ g L}^{-1}$, 67 kDa), immunoglobulin G (IgG, $\sim 10 \text{ g L}^{-1}$, heavy chain 50 kDa,
19 light chain 25 kDa)^[28] and transferrin ($\sim 2.6 \text{ g L}^{-1}$, 75 kDa)^[29]. Aside from that, for the Lutensol-
20 functionalized nanoparticles no differences between the individual nanoparticle samples with
21 different functionalization are visible. One of the most prominent bands visible in the nanoparticle
22 protein pattern is the band at $\sim 38 \text{ kDa}$, which can be assigned to the “stealth” protein clusterin
23 (apolipoprotein J). Additionally, another apolipoprotein can be found at around 28 kDa, which can
24 be assigned to apolipoprotein A1 (Apo A1). The presence and identification of these two main

1 proteins was recently confirmed for the same set of polystyrene nanoparticles with PEG
2 modifications via LC-MS experiments in our group and was thus expected for this system.^[22, 30, 31]

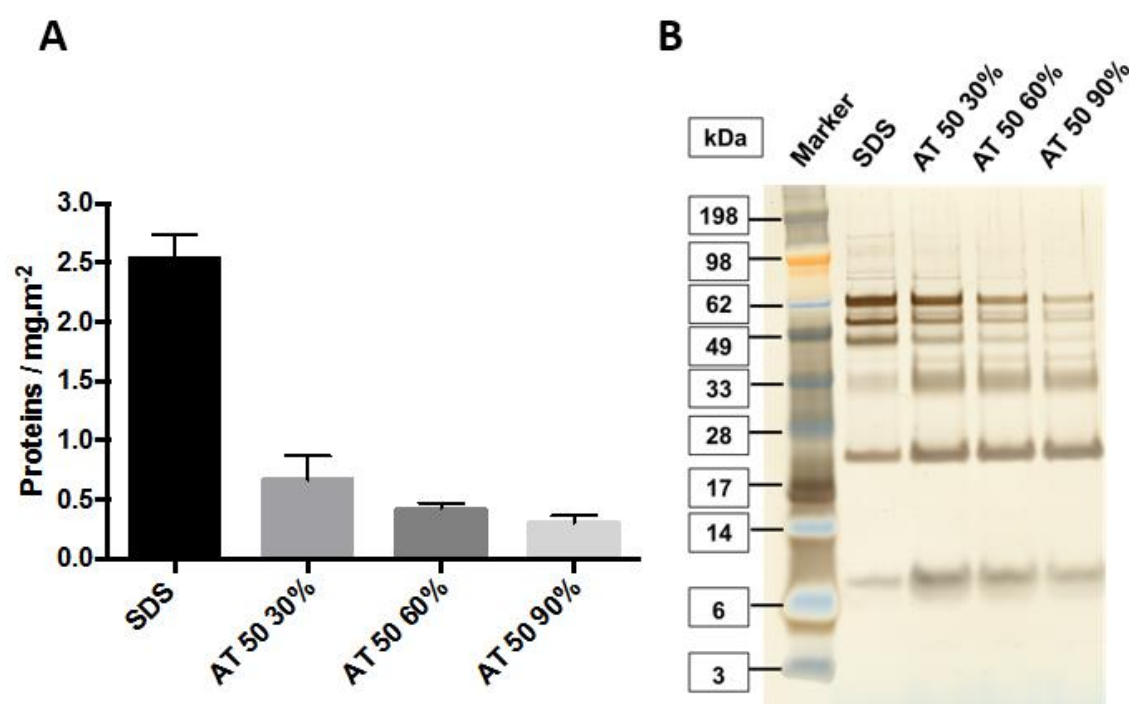
3 Since the PEG modification of the nanoparticles was performed *via* adsorption and not *via*
4 covalent functionalization, the fate of the surfactants after protein adsorption is important. While
5 the binding affinity of the surfactants possessing longer PEG chains (Lut AT50 and 80) is rather
6 high and in the same range as the binding affinities of most proteins ($\sim 10^6 \text{ M}^{-1}$), the two shorter
7 surfactant types are not bound as strong ($\sim 10^4 \text{ M}^{-1}$). This could in principle lead to surfactant
8 detachment and replacement by proteins. In case significant amounts of Lut would detach from the
9 nanoparticles, this would lead to the formation of macroscopic aggregates due to protein
10 denaturation, which was already examined in a previous study.^[32] In the case of Lut functionalized
11 NPs, this is not the case – independent from the type and concentration of surfactant – so that we
12 can conclude that the enrichment of stealth proteins is indeed due to the presence of Lut-based
13 surfactants on the nanoparticles.

14 In summary, the results shown in Figure 1 were not expected since previously it has been
15 well-investigated that increasing surface coverages of stealth functionalities have a profound
16 impact on the adsorption behavior of PEGylated nanoparticles. More specifically, increasing
17 surface coverages resulted in decreased protein adsorption.^[8, 33] To explain these unexpected
18 results, it is important to remember the strong affinity of Lut AT50 towards polystyrene
19 nanoparticles, because of which a significant amount of Lut AT50 is still present at the nanoparticle
20 surface after synthesis and extensive purification. It seems that the very small amount of Lut AT50
21 still present from the synthesis together with the adsorbed surfactant molecules is enough to cause
22 an enrichment of “stealth” proteins already, even though ITC measurements and ¹H-NMR
23 experiments evidence differences among the different samples used in this experiment. Any

1 additionally added PEG chains, whether long or short, did not further influence the protein
2 adsorption as far as observed from our experiments.

3 Since functionalizing Lut-prestabilized polystyrene nanoparticles with further Lut
4 surfactant molecules had no effect on protein corona formation so far, it was investigated whether
5 the protein corona pattern of Lut-prestabilized polystyrene nanoparticles can be tuned by the
6 addition of small amounts of SDS surfactant molecules. To this extent, the purified nanoparticles
7 were further functionalized using SDS according to surface coverages of 30%, 60% and 90% with
8 SDS surfactant molecules, assuming SDS occupies the same area on the nanoparticle surface as
9 Lut AT11. Indeed, the reported area per surfactant molecule of SDS is 0.56 nm^2 ,^[34] which is slightly
10 below the determined area for Lut AT11 (0.87 nm^2), but to make sure no excess of SDS was added,
11 they were assumed to be equal. To check for successful functionalization, zeta potential
12 measurements were executed. Since SDS is an anionic surfactant, the zeta potential values of Lut-
13 stabilized nanoparticles should decrease with increasing amounts of SDS added suggesting that
14 SDS was indeed adsorbed to the nanoparticle surface (Table S1.2). However, the protein assay and
15 SDS-PAGE analysis of SDS-functionalized Lut-stabilized polystyrene nanoparticles did not show
16 significant differences in protein adsorption when observed to the Lut-stabilized nanoparticles,
17 which indicates a dominant role of Lut AT50 over SDS concerning protein adsorption (Figure S7).
18 So far, from both conducted protein adsorption experiments, it could be concluded that the Lut
19 amount at the nanoparticle surface was already above the threshold where concentration
20 dependence can be detected. Therefore, the particle system used for further functionalization was
21 changed from Lut-stabilized to SDS-stabilized polystyrene nanoparticles, so that the particle
22 “starting” material is PEG chain free. The SDS-stabilized particles were purified until the minimum
23 amount for stable particles was obtained and further functionalized with different types of Lut

1 surfactants in different surface coverages according to the occupied surface areas determined for
2 each Lut surfactant. The purified SDS-stabilized particles were functionalized with Lut AT50
3 according to 30%, 60% and 90% surface coverage to first only vary the parameter of the PEG chain
4 length (Figure 2). These samples were characterized with respect to their hard protein corona
5 formation using a colorimetric protein assay and SDS-PAGE analysis as well as the zeta potential
6 before and after protein incubation (Table S1.3).



7
8 **Figure 3** Quantitative characterization of the hard protein corona pattern of SDS-stabilized Lutensol AT50-
9 functionalized polystyrene nanoparticles via a Pierce 660 nm protein assay (A) in combination with
10 qualitative analysis via SDS-PAGE (B). Proteins were detached from the nanoparticle surface after multiple
11 washing steps using an SDS Tris-HCl solution. Pure plasma (C) is given as reference.

12 The protein assay shows the same trend as observed for the first experiments with SDS-
13 stabilized polystyrene nanoparticles described above. Increasing surface coverages with Lut
14 surfactant molecules result in a decreased adsorbed protein amount. These results were
15 complemented by SDS-PAGE analysis. The protein patterns obtained depending on the surfactant

1 coverage differ significantly from each other. Notably, the adsorption of HSA (~ 67 kDa) and two
2 other proteins at ~ 55 kDa (antithrombin III) and ~ 48 kDa (apolipoprotein H), which are more
3 abundant in the non-functionalized samples as compared to the Lut-functionalized particles,
4 decreases significantly with higher Lutensol surface coverages. Moreover, the band that can be
5 attributed to clusterin (~ 38 kDa) is more visible in the Lut-functionalized samples thereby
6 indicating the strong enrichment in these samples. However, the amount of Lut present in the range
7 between 30% and 90% surface coverage seems not to influence the absolute amount of clusterin
8 adsorbed on the particles. It is worth mentioning that clusterin seems to be present in the SDS-
9 stabilized particles as well, which can be attributed to the strong tendency of many nanoparticles
10 to attract apolipoproteins in general.^[35, 36] However, its abundance was much less compared to the
11 stealth-functionalized nanoparticles. Additionally, the band at 28 kDa as well as the band at 8-10
12 kDa appears stronger compared to the particles without Lut. The 28 kDa band likely corresponds
13 to Apo A1, while the smaller bands need to be examined further.

14 In a second approach, the particles were functionalized to obtain a minimum number of
15 samples with a broad range of PEG chain density and length to estimate whether the effect on
16 protein adsorption stays the same as with only a varied density of AT50 or if it becomes more
17 pronounced: 1) AT11 functionalization according to 30% surface coverage, 2) AT25
18 functionalization corresponding to a surface coverage of 50%, 3) AT50 with a surface coverage of
19 70%, and 4) AT80 with a surface coverage of 90% of surfactant molecules. In contrast to the
20 purified SDS-stabilized polystyrene nanoparticles, the Lut-functionalized nanoparticles again
21 demonstrate a strong decrease in the adsorbed protein amount (Figure S8), however, between the
22 individual Lut functionalizations the difference is not significant. The trend as displayed in the
23 protein pattern (SDS-page) is also not significantly different from the one observed in Figure 2.

1 Comparable results were obtained for PEEP- and PEG-functionalized nanoparticles investigated
2 previously.^[8, 22] Interestingly, the decrease of the unspecific protein adsorption of high abundance
3 proteins is dependent on the surface area covered by PEG chains while the enrichment of lowly
4 abundant apolipoproteins, especially clusterin, seems to be constant. This is a very important
5 finding concerning the amount of PEG chains necessary for the optimum protein adsorption
6 patterns. To achieve enrichment of the stealth protein clusterin obviously a very low PEG chain
7 density is sufficient. However, for the decrease of the unspecific adsorption it seems to be the
8 optimum case when a very high PEG chain density close to full surface coverage can be reached.

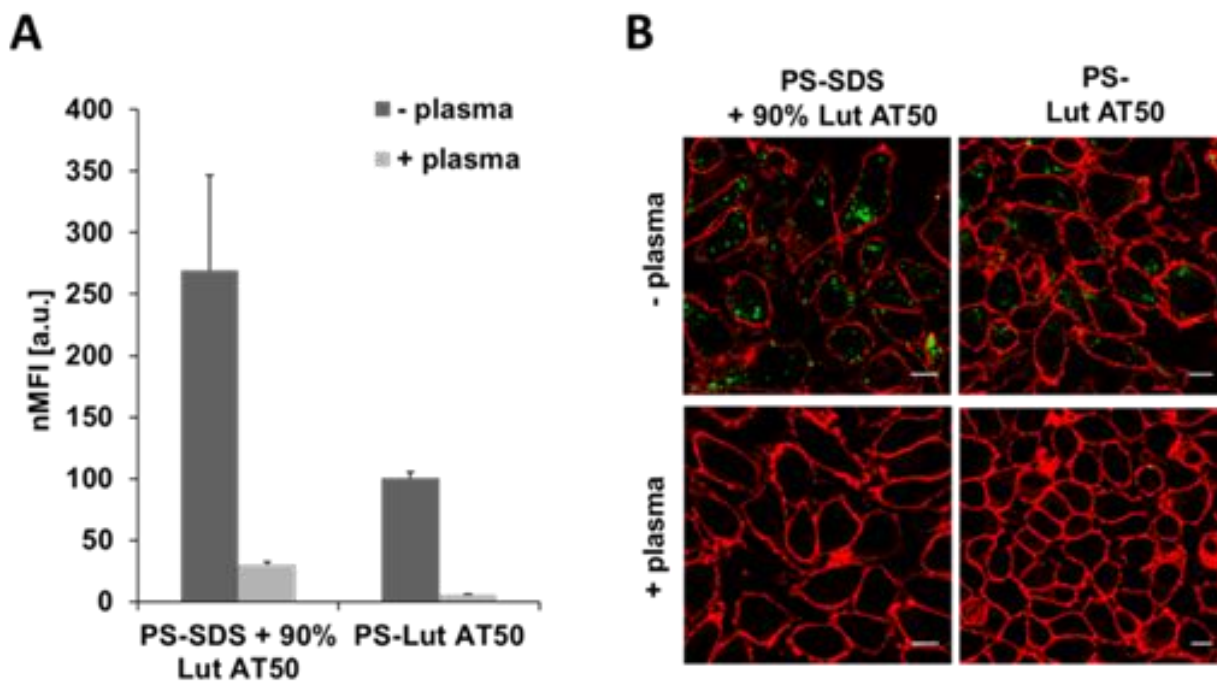
9

10 **Cellular uptake experiments**

11 Prolonged blood circulation is the major ability of stealth nanoparticles, and is caused by
12 reduced interactions with phagocytic cells (such as macrophages). Therefore, cellular interactions
13 with a murine macrophage-like cell line (RAW 264.7) were analyzed by flow cytometry and
14 confocal laser scanning microscopy (Figure 4) to investigate whether the obtained protein pattern
15 indeed resulted in a “stealth” behavior of the nanoparticles and to evaluate the corresponding
16 colloidal stability in a biological medium during cell uptake studies. Cellular uptake **in protein-free**
17 **cell medium** was tested for all SDS-stabilized polystyrene nanoparticles coated with Lut AT50
18 surfactant molecules with the different surface coverage and additionally with one sample with a
19 fully covered surface (referred to as PS-Lut AT50) **with and without NP incubation in plasma**
20 **before addition to the cells**. Notably, the PS-NPs with no or only small amounts of Lut (up to 60
21 % surface coverage) were not stable enough in the medium (**including prior plasma incubation of**
22 **NPs**) used for cell experiments and resulted in aggregation. Consequently, even though very small
23 amounts of PEG chains already result in the desired enrichment of stealth proteins, those amounts

1 are not enough to provide the needed colloidal stability. PS-NPs with 90% of surface coverage by
2 Lut AT50 as well as PS-NPs only stabilized with Lut AT50 (no SDS) as obtained after the synthesis
3 with only centrifugation step were sufficiently stable and could thus be analysed.

4



5

6

7 **Figure 4** Cellular uptake of Lut AT50-functionalized nanoparticles into RAW 264.7 macrophages. To
8 investigate the influence of corona formation, nanoparticles were incubated with human plasma for 1 h at
9 37 °C and the uptake compared to nanoparticles without plasma incubation. Cellular interaction was
10 quantitatively investigated using flow cytometry (A) and visualized by confocal laser scanning microscopy
11 (B). The median fluorescence intensity (MFI) was normalized based on the fluorescence intensity of each
12 nanoparticle (nMFI) and values are expressed as mean \pm SD of triplicates. Scale bar corresponds to 10 μ m.

13

14 In accordance with previous investigations by our group and others, the nanoparticles were highly
15 internalized in the absence of proteins (- plasma).^[8, 22] However, upon protein corona formation,

1 cellular interactions between the Lutensol-functionalized polystyrene nanoparticles and cells (+
2 plasma) were strongly diminished. In addition, the removal of SDS in the initial synthesis of the
3 nanoparticles reduced the cell uptake even further. Interestingly, this means that there are several
4 thresholds regarding the characteristics of PEG chains and their influence on the nanoparticle
5 properties. The smallest threshold seems to be the density of PEG chains needed to attract the
6 desired stealth proteins. This seems to happen as soon as any PEG is present, no matter which chain
7 length is applied. The second threshold seems to be the colloidal stability of the nanoparticles,
8 which in this case for Lutensol AT50 was between 60 and 90% surface coverage. The last threshold
9 (which is not a real threshold) concerns the reduction of unspecific protein adsorption and thus
10 unspecific cellular uptake, where the optimum was achieved with the highest possible surface
11 coverage.

12

13 **Experimental**

14 **Materials**

15 Particle synthesis, functionalization and characterization. Hexadecane (99%), dimethyl sulfoxide
16 (DMSO, 99.9%), sodium dodecyl sulfate (SDS, 99%), potassium chloride (KCl, 99%), and ethanol
17 (EtOH, 99.5%) were purchased from Sigma Aldrich (Munich, Germany). Lutensol AT11, 25, 50
18 and 80 surfactants (BASF, Ludwigshafen, Germany), styrene (99%, Merck, Darmstadt, Germany),
19 2,2'-azobis(2-methylbutyronitrile) (V59, Wako Chemicals, Japan) and deuterium oxide (D₂O,
20 99.8%, Roth, Karlsruhe, Germany). Styrene was filtered through a column of aluminum oxide and
21 stored at 4 °C until use for the synthesis of nanoparticles. The fluorescent dye, Bodipy-1, which is
22 a polymerizable derivative of borondipyrromethene was synthesized in house according to the
23 reference.^[37] Lutensol is a polymeric surfactant consisting of a hydrophilic PEG block (numbers

1 11, 25, 50 and 80 indicate the nominal degree of ethoxylation) and a C16-C18 hydrophobic
2 saturated fatty alcohol.

3

4 **Protein corona formation and cell experiments.**

5 Dithiotreitol (DTT, 99%), iodoacetamide (IAA, 99%), hydrochloric acid (HCl, 99.9%), bovine
6 serum albumin (BSA, 96%), acetic acid (AA, 99.85%) and formic acid (FA, 95%) were purchased
7 from Sigma Aldrich (Munich, Germany). Phosphate-buffered saline (PBS), acetic acid glacial and
8 NuPAGE® MES SDS running buffer (MES) were purchased from Thermo Fischer Scientific
9 (Waltham, USA). Ultrapure water was obtained from Brown (Melsungen, Germany) and ULC-MS
10 water from Biosolve BV (Valkenswaard, the Netherlands). The Pierce 660 nm protein assay,
11 protein reagent and Silver Staining kit are commercially available from Thermo Fischer Scientific
12 (Rockford, USA) and were used according to manual's instructions.

13

14 **Plasma source.** Blood from 10 healthy donors was taken after obtaining informed consent and
15 approval of the study by the local ethics committee. Sodium citrate was added to the donated blood
16 to prevent clotting and plasma was separated by centrifugation. The plasma was pooled and
17 aliquots were stored at -80 °C. After thawing, the plasma was centrifuged at 20000 g (14400 rpm)
18 for 30 min to remove any residual protein precipitates. With the Pierce 660 nm protein assay a
19 protein concentration of 66 mg mL⁻¹ was determined.

20

21 **Methods**

22 **Nanoparticle Synthesis**

1 Model polystyrene nanoparticles were prepared by radical polymerization in miniemulsion as
2 described previously.^[34, 38] Thus, for SDS-stabilized polystyrene nanoparticles, 74 mg of SDS was
3 dissolved in 24 mL deionized water. Simultaneously, 98 mg of the initiator V59 and 323 μ L of
4 hexadecane were dissolved in 6 g of purified styrene. For Lutensol-stabilized polystyrene
5 nanoparticles two different batches were prepared (one with and one without Bodipy-1). In short,
6 1000 mg and 600 mg of Lutensol AT50 surfactant were dissolved in respectively, 120 mL and 24
7 mL deionized water. For the first, 1250 mg hexadecane together with 450 mg V59 were dissolved
8 in 30 g purified styrene. For the latter, 250 mg hexadecane, 100 mg V59 and 6 mg Bodipy-1 were
9 dissolved in 6 g of purified styrene. After separate preparation of the two phases, they were
10 combined and stirred for 1 h at room temperature for pre-emulsification. Afterwards, the mixture
11 was homogenized using a microfluidizer setup (LM10 High Shear Fluid Processor, IDEX Material
12 Processing, Westwood, USA), according to the following parameters: Y chamber and a pressure
13 of 15000 psi. Then, the polymerization was carried out for 16 h at 72 °C. After synthesis, the
14 nanoparticles were filtered through Kimtech wipes (Kimberly-Clark, USA) before starting the
15 extensive cleaning procedure. The Lutensol-stabilized polystyrene nanoparticles were purified nine
16 times by repetitive centrifugation/redispersion steps (13000 rpm, 60 min, Sigma 3k-30) in
17 demineralized water and/or a mixture of 5:1 water/EtOH. The SDS-stabilized nanoparticles were
18 purified by dialysis for 72 h, refreshing the water each 8 h.

19

20 **Nuclear Magnetic Resonance (NMR) Spectroscopy**

21 ¹H-NMR spectra were recorded on a Bruker AVANCE 250 MHz spectrometer. All spectra were
22 measured in deuterium oxide (D₂O), using dimethyl sulfoxide (DMSO) as an internal standard,

1 with 16 scans per sample under a 12 s pulse delay. For these experiments, the relative concentration
2 of D₂O, DMSO and nanoparticle dispersion was kept constant.

3

4 **Surface Tension Measurements**

5 Surface tension measurements were carried out with a DCAT 21 tensiometer from DataPhysics
6 Instruments (Filderstadt, Germany).

7

8 **Scanning Electron Microscopy (SEM)**

9 SEM images were recorded by using a field emission microscope (LEO (Zeiss) 1530 Gemini,
10 Oberkochen, Germany) operated with an accelerating voltage of 120 V. A droplet of nanoparticle
11 dispersion (solid content of about 0.01 wt%) was placed onto a silica wafer and dried under ambient
12 conditions.

13

14 **Dynamic Light Scattering (DLS)**

15 Size distributions of the nanoparticle dispersions and nanoparticle-protein corona complexes were
16 determined on an ALV spectrometer (ALV, Langen, Germany) consisting of a goniometer and an
17 ALV-5004 multiple-tau full-digital correlator (320 channels) allowing measurements over an
18 angular range from 30 to 150°. As light source a He-Ne laser (JDS Uniphase, Milpitas, USA)
19 working at an output power of 25 mW and a wavelength of 632.8 nm was utilized. For light
20 scattering experiments, pure nanoparticle samples were filtered through 0.45 µm Millex LCR
21 filters (Millipore) into cylindrical quartz cuvettes with an outer diameter of 20 mm (Hellma,

1 Müllheim, Germany). The cuvettes were cleaned by dust-free distilled acetone in a special acetone
2 fountain prior to use in experiments. For the size determination of the nanoparticles, they were
3 diluted in MilliQ water to a concentration of 0.01 mg mL⁻¹. The nanoparticles were analyzed
4 according to the CONTIN algorithm^[39, 40] and the obtained diffusion coefficients for each
5 scattering vector q were extrapolated to $q \rightarrow 0$. The extrapolated D_z was converted into the R_h
6 applying Stokes law ($R_h = k_B T / 6\pi\eta D$; R_h is the hydrodynamic radius, while k_B , T , η and D
7 represent the Boltzmann constant, temperature, viscosity and diffusion coefficient, respectively).

8

9 **Zeta Potential Measurements**

10 The zeta potential of nanoparticles (in the presence and absence of proteins) was measured in 10⁻³
11 M KCl solution using a Zetasizer Nano Z (Malvern Instruments GmbH, Herrenberg, Germany) at
12 20 °C. An aqueous nanoparticle suspension (0.05 mg mL⁻¹) was mixed with 1 mL of freshly thawed
13 human citrate plasma (total protein concentration 66 g L⁻¹). After 1 h of mild shaking in a sample
14 shaker at 37 °C, the sample was centrifuged for 1 h at 20000 g (14400 rpm) and 4 °C. Afterwards,
15 the nanoparticles were separated from the supernatant and the pellet was resuspended in phosphate-
16 buffered saline (PBS). The suspension was centrifuged for 1 h at 20000 g (14400 rpm) and 4 °C.
17 These washing steps were repeated for a total of three times. Before the last washing step, the
18 suspension was transferred into a new Eppendorf-tube. After the last washing step, the pellet was
19 resuspended in demineralized water. 20 µL of each sample was diluted with 1 mL of 1 M KCl
20 solution and directly measured at 20 °C after two minutes of equilibration. Each measurement was
21 repeated three times; mean values and standard deviations were calculated.

22

1 **Isothermal Titration Calorimetry**

2 The calorimetric measurements were performed using a NanoITC Low Volume (TA Instruments,
3 Eschborn, Germany) with an effective cell volume of 170 μL . In an experiment 50 μL of a Lutensol
4 AT type surfactant solution was titrated to 300 μL of a suspension of polystyrene nanoparticles.
5 The experimental temperature was kept constant at 25 $^{\circ}\text{C}$. Additionally, the same amount of each
6 surfactant solution was titrated into pure water to determine the heat of dilution as reference. The
7 number and injected volume of the titration steps were kept the same for all measurements (25 x 2
8 μL). The spacing between the injections was set to 300 s. The integrated reference heats were then
9 subtracted from the integrated heats of the adsorption experiments. The normalized heats were
10 subsequently analyzed with a fitting procedure according to an independent binding model^[41] using
11 the software NanoAnalyze, version 3.5.0 by TA Instruments, to obtain the association constant
12 (K_a), the reaction enthalpy (ΔH) and the reaction stoichiometry n as the fitting parameters. For the
13 experiments, the following concentrations were used: $2.1 \cdot 10^6$ mM polystyrene nanoparticle
14 dispersion were titrated with 5.4 mM Lutensol AT11, $3.2 \cdot 10^6$ mM particle dispersion were titrated
15 with 2.9 mM Lutensol AT25, $1.2 \cdot 10^5$ mM particle dispersion were titrated with 1.6 mM Lutensol
16 AT50 and $4.3 \cdot 10^6$ particle dispersion were titrated with 0.5 mM Lutensol AT80.

17

18 **Protein Corona Formation**

19 For protein corona experiments, the ratio of plasma volume to total particle surface area was kept
20 constant at 20 mL m^{-2} to ensure reproducibility. The particle surface area was kept constant at 0.05
21 m^2 by diluting the nanoparticle dispersions to a total volume of 300 μL . To allow protein corona
22 formation, the nanoparticle dispersions were incubated with 1 mL citrate-stabilized human plasma

1 for 1 h at 37 °C under constant agitation. The particles were separated from the supernatant by
2 centrifugation at 20 000 g (14400 rpm) for 1 h. Afterwards, the nanoparticles were washed with
3 PBS in three centrifugation steps at 20 000 g (14400 rpm) for 1 h to maintain solely the hard corona.
4 To elute the adsorbed proteins, the particle pellet was resuspended in 100 µL of an aqueous solution
5 with 2% (w/v) SDS and 62.5 mM Tris-HCl and incubated at 95 °C for 5 min. After this procedure,
6 the nanoparticles were again pelleted and the supernatant was used for protein quantification, SDS-
7 PAGE and LC-MS.

8

9 **Pierce 660 nm Protein Assay**

10 Protein concentrations were determined using a Pierce 660 nm protein assay (Thermo Scientific,
11 Rockford, USA) following manufacturer's instructions using BSA as standard. The ready-to-use
12 Pierce® 660 nm protein assay reagent was supplied with 1 g of ionic detergent compatibility
13 reagent. Each sample was measured in triplicate.

14

15 **Sodium Dodecyl Sulfate Polyacrylamide Gel Electrophoresis (SDS-PAGE)**

16 16.25 µL (1 µg protein per lane) of each protein sample was mixed with 6.25 µL NuPAGE LDS
17 Sample Buffer and 2.5 µL NuPAGE Sample Reducing Agent and incubated for 10 min at 70 °C.
18 Subsequently, the samples were loaded onto a NuPAGE® 10% Bis-Tris gel (Thermo Fischer
19 Scientific) and subjected to SDS-PAGE according to standard procedures. The electrophoresis was
20 carried out for 90 min at 100 V in NuPAGE MES SDS Running Buffer. As molecular marker, 10
21 µL SeeBlue Plus2 Pre-Stained Standard (Thermo Fischer Scientific) was added. Finally, the
22 proteins were visualized using Pierce Silver Stain kit according to the instruction manual.

1

2 **Cell Culture**

3 The murine macrophage cell line RAW264.7 was cultured in Dulbecco's modified eagle medium
4 (DMEM), supplemented with 10% fetal calf serum (FCS), 100 U mL⁻¹ penicillin, 100 mg mL⁻¹
5 streptomycin and 2 mM glutamine. Cells were grown in a humidified incubator at 37 °C and 5%
6 CO₂.

7

8 **Flow Cytometry**

9 For the quantitative analysis of nanoparticle uptake into cells flow cytometry measurements were
10 conducted. 1 x 10⁵ cells per mL (RAW 264.7) were allowed to attach in six-well plates. After 12
11 h the cells were washed with DPBS to remove all proteins from FBS and kept in DMEM without
12 additional proteins. Nanoparticles were incubated with human citrated plasma as described above
13 (protein corona formation), centrifuged to remove unbound proteins and added at a concentration
14 of 25 µg mL⁻¹ to the cells. After 2 h of nanoparticle incubation, adherent cells were detached from
15 the culture vessel in 2.5% trypsin (Gibco, Germany) and washed with magnesium- and calcium-
16 free PBS (Gibco, Germany). Flow cytometry measurements were performed on a CyFlow ML
17 Cytometer, the FL1 channel (excited with a 488 nm laser line, emission filter 527 ± 12 nm) was
18 used to analyze the uptake of nanoparticles (Bodipy-labeled). Data analysis was performed using
19 FCS Express V4 software by selecting the cells on a forward/sideward scatter plot, thereby eluding
20 cell debris. These gated events were further analyzed by the amount of fluorescent signal expressed
21 as median intensity. The median in FL1 was determined from 1D histograms, demonstrating the

1 number of nanoparticles taken up or associated with individual cells. Mean values and standard
2 deviations were determined from triplicates.

3 As different nanoparticles contained different amounts of dye, the fluorescence intensity for each
4 particle was measured with a Tecan Infinite R M1000 PRO microplate reader with standard settings
5 of the software iControl® at an excitation and emission wavelength of respectively 523 and 536
6 nm. The fluorescence intensity values of each nanoparticle (FINP) were further normalized
7 (nFINP) to the fluorescence intensity value for polystyrene nanoparticles (FIPS) to further
8 normalize the median fluorescence intensity (MFI) obtained from flow cytometry measurements.
9 The following equations were used:

$$10 \quad nFI_{NP} = \frac{FI_{NP}}{FI_{PS}}$$

$$11 \quad nMFI = \frac{MFI}{nFI_{NP}}$$

12

13 **Confocal Laser Scanning Microscopy (CLSM)**

14 1×10^5 cells per mL (RAW 264.7) were seeded in Ibidi iTreat μ -dishes (IBIDI, Germany) for 24
15 h, washed with PBS and kept in DMEM without additional proteins. $25 \mu\text{g mL}^{-1}$ pre-incubated
16 nanoparticles were added to cells for 2 h. Afterwards cells were washed with PBS three times and
17 stained with CellMask Orange (CMO, stock solution: 5 mg mL^{-1} in DMSO, Invitrogen, USA)
18 which labeled the cell membrane red. CMO ($0.2 \mu\text{L}$) was diluted with one mL of Hanks' Balanced
19 Salt solution (HBSS, Life Technologies, USA). After adding the diluted staining solution ($400 \mu\text{L}$)
20 to cells, live cell images were taken on a Leica TCS SP5 II microscope with an HC PL APO CS
21 $63\times/1.4$ oil objective using the software LAS AF 3000 software. The fluorescence signals of

1 nanoparticles (excitation: 488 nm, pseudo colored green) and CMO (excitation: 561 nm, pseudo
2 colored red) were detected in a serial scan mode.

3 **Conclusions**

4 Our results reported here demonstrate that surface functionalization of polystyrene nanoparticles
5 via the physical adsorption of PEGylated (Lutensol) surfactants significantly reduces unspecific
6 protein adsorption. When Lutensol was used already as a stabilizing surfactant during the synthesis
7 of the nanoparticles, the small amount remaining on the surface after purification was already
8 enough to result in a significantly reduced unspecific protein adsorption and enrichment of stealth
9 proteins. Even a subsequent addition of sodium dodecyl sulfate did not alter this behavior.
10 However, when nanoparticles prestabilized with sodium dodecyl sulfate were used, it could be
11 demonstrated that the unspecific protein adsorption decreased with increasing PEG chain density.
12 Interestingly, already the smallest introduced amounts of PEG chains already resulted in a
13 recruitment of the stealth proteins clusterin and ApoA1. When further varying the PEG chain
14 length, no variation of this trend was found, so that the two factors do not seem to cause consecutive
15 effects. To prevent aggregation and to enhance colloidal stability of the nanoparticles in biological
16 media the results indicated that a full surface coverage of the nanoparticle with PEG functionalities
17 is beneficial and results in least uptake by macrophages. Altogether, it became clear that several
18 thresholds regarding the effects of PEG chain modification exist. In future studies, we would
19 recommend to achieve the highest functionalization density possible to yield the best performance
20 for the desired applications.

21

22 **Conflicts of interest**

1 There are no conflicts to declare.

2 **Acknowledgements**

3 The authors wish to thank K. Klein and A. Schoth for helping with the synthesis of nanoparticles
4 and G. Glasser for acquiring electron microscopy images. Funding by the DFG Collaborative
5 Research Research Center 1066 is acknowledged by C. Weber and J. Simon. S. Seneca was
6 supported by an Erasmus Scholarship from the European Commission. A. Ethirajan was a FWO
7 (Fonds Wetenschappelijk Onderzoek) postdoctoral fellow during the execution of this project.

8 **Keywords**

9 nanocarriers; protein corona; stealth effect; poly(ethylene glycol); surfactants

10 **References**

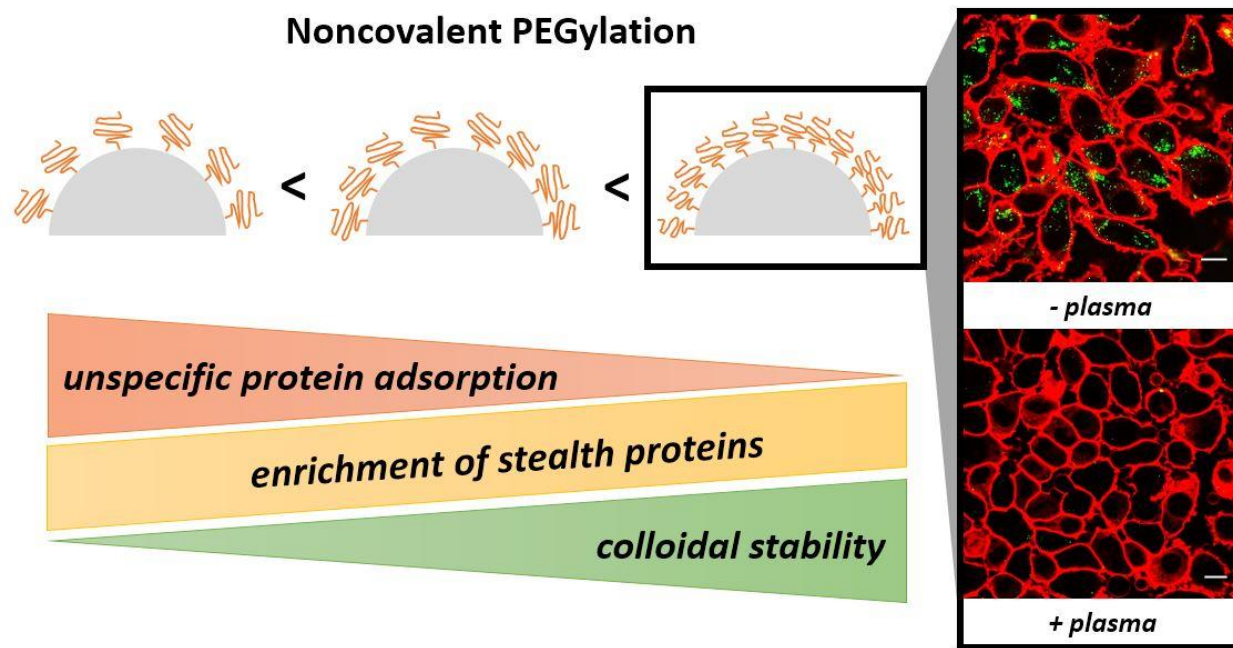
- 11 [1] T. Cedervall, I. Lynch, M. Foy, T. Berggard, S. C. Donnelly, G. Cagney, S. Linse, K. A. Dawson, *Angew*
12 *Chem Int Ed Engl* **2007**, *46*, 5754.
- 13 [2] S. Tenzer, D. Docter, J. Kuharev, A. Musyanovych, V. Fetz, R. Hecht, F. Schlenk, D. Fischer, K. Kiouptsi,
14 C. Reinhardt, K. Landfester, H. Schild, M. Maskos, S. K. Knauer, R. H. Stauber, *Nature nanotechnology*
15 **2013**, *8*, 772.
- 16 [3] C. M. Hu, R. H. Fang, B. T. Luk, L. Zhang, *Nanoscale* **2014**, *6*, 65.
- 17 [4] F. M. Veronese, G. Pasut, *Drug Discov Today* **2005**, *10*, 1451.
- 18 [5] H. Otsuka, Y. Nagasaki, K. Kataoka, *Adv Drug Deliv Rev* **2003**, *55*, 403.
- 19 [6] C. Sacchetti, K. Motamedchaboki, A. Magrini, G. Palmieri, M. Mattei, S. Bernardini, N. Rosato, N.
20 Bottini, M. Bottini, *Acs Nano* **2013**, *7*, 1974.
- 21 [7] S. N. S. Alconcel, A. S. Baas, H. D. Maynard, *Polym Chem-Uk* **2011**, *2*, 1442.
- 22 [8] S. Schottler, G. Becker, S. Winzen, T. Steinbach, K. Mohr, K. Landfester, V. Mailander, F. R. Wurm, *Nat*
23 *Nanotechnol* **2016**, *11*, 372.
- 24 [9] S. Schottler, K. Landfester, V. Mailander, *Angew Chem Int Ed Engl* **2016**, *55*, 8806.
- 25 [10] R. Gref, M. Luck, P. Quellec, M. Marchand, E. Dellacherie, S. Harnisch, T. Blunk, R. H. Muller, *Colloids*
26 *Surf B Biointerfaces* **2000**, *18*, 301.
- 27 [11] R. Michel, S. Pasche, M. Textor, D. G. Castner, *Langmuir* **2005**, *21*, 12327.
- 28 [12] C. D. Walkey, J. B. Olsen, H. Guo, A. Emili, W. C. Chan, *J Am Chem Soc* **2012**, *134*, 2139.
- 29 [13] J. L. Perry, K. G. Reuter, M. P. Kai, K. P. Herlihy, S. W. Jones, J. C. Luft, M. Napier, J. E. Bear, J. M.
30 DeSimone, *Nano Lett* **2012**, *12*, 5304.
- 31 [14] A. Vonarbourg, C. Passirani, P. Saulnier, J. P. Benoit, *Biomaterials* **2006**, *27*, 4356.
- 32 [15] R. Bartucci, M. Pantusa, D. Marsh, L. Sportelli, *Biochim Biophys Acta* **2002**, *1564*, 237.
- 33 [16] N. Bertrand, P. Grenier, M. Mahmoudi, E. M. Lima, E. A. Appel, F. Dormont, J. M. Lim, R. Karnik, R.
34 Langer, O. C. Farokhzad, *Nature Communications* **2017**, *8*.

- 1 [17] M. Malmsten, K. Emoto, J. M. Van Alstine, *Journal of Colloid and Interface Science* **1998**, *202*, 507.
2 [18] P. M. Antonik, A. M. Eissa, A. R. Round, N. R. Cameron, P. B. Crowley, *Biomacromolecules* **2016**, *17*,
3 2719.
4 [19] S. I. Jeon, J. D. Andrade, *Journal of Colloid and Interface Science* **1991**, *142*, 159.
5 [20] S. I. Jeon, J. H. Lee, J. D. Andrade, P. G. Degennes, *Journal of Colloid and Interface Science* **1991**, *142*,
6 149.
7 [21] H. Lee, R. G. Larson, *Biomacromolecules* **2016**, *17*, 1757.
8 [22] J. Müller, K. N. Bauer, D. Prozeller, J. Simon, V. Mailänder, F. R. Wurm, S. Winzen, K. Landfester,
9 *Biomaterials* **2017**, *115*, 1.
10 [23] T. Wolf, T. Steinbach, F. R. Wurm, *Macromolecules* **2015**, *48*, 3853.
11 [24] T. Steinbach, F. R. Wurm, *Angew Chem Int Edit* **2015**, *54*, 6098.
12 [25] S. Winzen, J. C. Schwabacher, J. Müller, K. Landfester, K. Mohr, *Biomacromolecules* **2016**, *17*, 3845.
13 [26] S. Schöttler, K. Klein, K. Landfester, V. Mailänder, *Nanoscale* **2016**, *8*, 5526.
14 [27] S. Winzen, S. Schoettler, G. Baier, C. Rosenauer, V. Mailänder, K. Landfester, K. Mohr, *Nanoscale*
15 **2015**, *7*, 2992.
16 [28] A. Gonzalez-Quintela, R. Alende, F. Gude, J. Campos, J. Rey, L. M. Meijide, C. Fernandez-Merino, C.
17 Vidal, *Clin Exp Immunol* **2008**, *151*, 42.
18 [29] A. Helander, *Clin Chem* **1999**, *45*, 131.
19 [30] S. Schöttler, G. Becker, S. Winzen, T. Steinbach, K. Mohr, K. Landfester, V. Mailänder, F. R. Wurm,
20 *Nat Nano* **2016**, *11*, 372.
21 [31] L. K. Müller, J. Simon, C. Rosenauer, V. Mailänder, S. Morsbach, K. Landfester, *Biomacromolecules*
22 **2018**, *19*, 374.
23 [32] S. Winzen, J. C. Schwabacher, J. Müller, K. Landfester, K. Mohr, *Biomacromolecules* **2016**, *17*, 3845.
24 [33] D. F. Marruecos, M. Kastantin, D. K. Schwartz, J. L. Kaar, *Biomacromolecules* **2016**, *17*, 1017.
25 [34] K. Landfester, N. Bechthold, F. Tiarks, M. Antonietti, *Macromolecules* **1999**, *32*, 2679.
26 [35] K. Mohr, *Journal of Nanomedicine & Nanotechnology* **2014**, *05*.
27 [36] S. Ritz, S. Schöttler, N. Kotman, G. Baier, A. Musyanovych, J. Kuharev, K. Landfester, H. Schild, O.
28 Jahn, S. Tenzer, V. Mailänder, *Biomacromolecules* **2015**, *16*, 1311.
29 [37] I. Garcia-Moreno, A. Costela, L. Campo, R. Sastre, F. Amat-Guerri, M. Liras, F. L. Arbeloa, J. B. Prieto,
30 I. L. Arbeloa, *J Phys Chem A* **2004**, *108*, 3315.
31 [38] K. Landfester, N. Bechthold, F. Tiarks, M. Antonietti, *Macromolecules* **1999**, *32*, 5222.
32 [39] S. W. Provencher, *Makromol Chem* **1979**, *180*, 201.
33 [40] S. W. Provencher, *Comput Phys Commun* **1982**, *27*, 229.
34 [41] E. Freire, O. L. Mayorga, M. Straume, *Anal Chem* **1990**, *62*, A950.

35

1 **Table of Contents**

2
3 The influence of noncovalent PEGylation on nanocarriers was characterized with regard to PEG chain
4 density and length. It was found that the enrichment of stealth proteins did not depend on either of the
5 variables, but concentration thresholds regarding colloidal stability and unspecific protein adsorption have
6 to be taken into account.



7